2—must be taken as a change in the generic model as defined in eq 5 and can therefore indeed increase work output.

As a last example consider the two reservoirs to contain chemical substances which can react, e.g., according to

$$H_2 + {}^1/_2O_2 \rightleftharpoons H_2O \tag{61}$$

The substances need not be spatially separated. Then the temperatures of Figure 3 translate into chemical potentials or, for simplicity, into concentrations c_α. Each engine is a chemical half-reaction

$$H_2 \rightleftharpoons 2H^+ + 2e^- \tag{62a}$$

$$\begin{gathered} {}^1/_2O_2 + 2e^- \rightleftharpoons O^{2-} \\ (\text{or } {}^1/_2O_2 + 2e^- + H_2O \rightleftharpoons 2OH^-) \end{gathered} \tag{62b}$$

which operates reversibly. If the process is heterogeneous as in a typical fuel cell, the resistors represent diffusion to and from the catalytic surfaces according to Fick's law

$$j_\alpha = D_\alpha(c_\alpha' - c_\alpha) \tag{63}$$

for each substance α, where D_α is the diffusion constant and c_α' and c_α are the concentrations on the catalytic surface and in the reaction mixture, respectively. In the example above c_{H^+} and c_{OH^-} are considered to be their equilibrium values represented by the environment. Note that eq 63 is completely analogous to the thermal equation 40. The relaxation resistor κ represents uncatalyzed (uncaptured) reaction between the reactants. Looked at this way our model describes how to obtain the most energy from, e.g., a fuel cell in time τ. If energy is no objective, but one wants a reaction of the type

$$A + B \rightleftharpoons C + D \tag{64}$$

consider it implemented as two pairs of half-reactions back to back such that the work output of one drives the other. The description using half-reactions is purely to emphasize the analogy with the thermal treatment in the previous sections. Finite-time availability is just as important in homogeneous reactions, and we believe that the notion of nonvanishing rate will be very useful for designing and describing chemical reactions in general.

Acknowledgment. Part of this work was performed while M.H.R. was on sabbatical visits to the University of Chicago and the University of Copenhagen. He wishes to express his gratitude to his hosts at both institutions and to the National Science Foundation and the Danish Science Foundation for their financial support. B.A. wants to thank NATO for a travel grant. Part of this work was carried out at the Aspen Center for Physics, whose hospitality we appreciate. We thank Peter Salamon for his helpful comments.

Appendix

Extrapolation Procedure to Initial State. As mentioned in section VIB, the optimal control problem has to be solved backward from a guessed final state even though it is the initial state which is specified. In order to find that final-state $\mathbf{T}_f$ whose optimal trajectory was less than a prescribed distance from the desired initial-state $\mathbf{T}_i$ a time τ earlier, a simple linear two-dimensional extrapolation procedure was set up.

First a nonoptimal trajectory was integrated from $\mathbf{T}_i$ for time τ to obtain an estimate of $\mathbf{T}_f$ which, along with two other points in the vicinity of this estimate, formed starting points from which optimal trajectories were calculated backward. Two-dimensional extrapolation in $\mathbf{T}_i$ from these initial states with replacement of the trajectory which was furthest away from $\mathbf{T}_i$ was repeated until the error was less than a prescribed value.

Vibrational Predissociation of H_2–, D_2–, and HD–Ar van der Waals Molecules

Jeremy M. Hutson,† Christopher J. Ashton,‡ and Robert J. Le Roy*

Guelph-Waterloo Centre for Graduate Work in Chemistry, University of Waterloo, Waterloo, Ontario N2L 3G1, Canada
(Received: December 22, 1982; In Final Form: March 15, 1983)

Accurate close-coupling calculations are peformed for vibrationally predissociating states of H_2–Ar, D_2–Ar, and HD–Ar, using the best potential energy surface available. All the states examined have very small widths ($\Gamma << 10^{-6}$ cm^{-1}, corresponding to lifetimes >20 μs). There is a pronounced tendency for predissociation to yield rotationally hot diatomic molecules, even for the H_2–Ar and D_2–Ar complexes where the present potential has no anisotropic terms of higher order than $P_2(\cos\theta)$. This near-resonant effect is particularly strong for HD–Ar, where all Legendre terms are present in the potential; in this case, about 50% of the HD products are formed in the highest two accessible rotational levels. There is some evidence for a rotational rainbow effect in the product rotational state distributions. Perturbation theory calculations which attempt to reproduce the accurate calculations are also reported. They successfully model the qualitative features of the close-coupling results, but are not quantitatively accurate even for these weakly coupled systems. It appears that this inadequacy is due to the need for a very accurate representation of the bound state wave function and to the neglect of important couplings between the different open channels. This conclusion is supported by the observation that very large basis sets are required to obtain convergence of the close-coupling calculations.

1. Introduction

van der Waals molecules whose monomers are internally excited often have enough energy to predissociate, and may do so by several mechanisms. Of particular interest here is vibrational predissociation (VP), where internal vibrational energy of one of the monomers is converted into rotational and/or translational energy of the fragments.

† NATO Postdoctoral Research Fellow.
‡ Present address: Chemistry Department, Brookhaven National Laboratory, Upton, NY 11973.

0022-3654/83/2087-2713$01.50/0

The lifetimes and spectroscopic line widths due to this process are important when designing experiments to observe van der Waals molecules, since some detection systems rely on lifetimes lying within a particular range. Moreover, if VP lifetimes or product state distributions can be measured, they should give valuable information about the dependence of the intermolecular potentials on monomer internal vibration. However, it should be noted that van der Waals molecules involving rotationally excited monomers may be able to predissociate by converting rotational energy into translation, and when allowed this process is usually much faster than VP.

Several groups have reported experimental results on VP,[1,2] and this has stimulated a good deal of theoretical work.[3-5] However, this work has relied mainly on model potentials of unknown quality and approximate dynamical treatments of unknown reliability. The purpose of this paper is to report accurate calculations for vibrationally predissociating levels of H_2–Ar, D_2–Ar, and HD–Ar, for which quantitative information about the dependence of the intermolecular potential on the diatom stretching coordinate has been obtained by Carley and Le Roy[6] from the spectroscopic data of McKellar and Welsh.[7] These accurate calculations will then be compared with the results of perturbation theory, which will be shown to be seriously inaccurate for these systems. Our results will also be compared with the results of Kidd and Balint-Kurti,[8] who have performed accurate calculations of photodissociation in H_2–Ar using Shapiro's artificial channel method.[9]

We chose to study the isotopic H_2–Ar complexes not only because of the availability of a reliable potential surface, but also because the physics of VP in these systems is particularly interesting. Previous approximate theoretical work on VP[3-5] has emphasized two main features:

(i) If most or all of the diatom vibrational energy released flows into intermolecular translation, it is suggested that a "momentum gap" effect will lead to the VP widths for these systems being very small indeed, of the order of 10^{-7} to 10^{-12} cm^{-1}. The origin of this effect is in oscillatory cancellation in the radial overlap integrals appearing as multiplicative factors in perturbative expressions for the widths. The greater the final intermolecular momentum, the more oscillatory will be the product state intermolecular continuum wave function, and the smaller will be the width. For the H_2–Ar systems, the diatom releases about 4000 cm^{-1} of vibrational energy to break up a complex bound by only about 25 cm^{-1}, and the oscillatory cancellation effect is predicted to be large.

(ii) There is the possibility of partial absorption of the released vibrational energy into diatom rotation. Because less energy would then go into intermolecular translation, the momentum gap effect would be lessened and the total VP widths might be larger. However, a "near-resonant" process of this kind requires a relatively large change in diatom rotational quantum number during predissociation. In a diabatic formulation of the problem, the *direct* bound–continuum potential couplings which enable such a process to occur arise from high-order terms in the Legendre expansion of the anisotropy of the intermolecular potential, and as such would be rather weak. It is thus possible that higher-order, indirect potential couplings might play a crucial role in determining the importance of this process. Although some of the earlier work has considered direct near-resonant effects,[5] the importance of indirect effects has never been investigated.

By performing both accurate and perturbative calculations on VP in these systems, we hoped both to clarify the relative importance of momentum gap and near-resonant effects and to explore the factors determining this balance.

2. The Potential Energy Surface

The calculations in this paper were performed with the $BC_3(6, 8)$ H_2–Ar potential of Carley and Le Roy.[6] This is expanded in the form

$$V(R,\xi,\theta) = \sum_{k=0}^{3} \sum_{\lambda=0,2} \xi^k P_\lambda(\cos j) V_{\lambda k}(R)$$

where R is the distance between the atom and the diatom center of mass, the diatom bond length is represented by the stretching coordinate $\xi = (r - r_0)/r_0$ with $r_0 = 0.7666438$ Å, and θ is the angle between **R** and the axis of the diatom. The radial strength functions $V_{\lambda k}(R)$ all have the form

$$V_{\lambda k}(R) = A^{\lambda k} \exp(-\beta_\lambda R) - D(R)[C_6{}^{\lambda k}/R^6 + C_8{}^{\lambda k}/R^8]$$

where

$$D(R) = \exp[-4(R_0/R - 1)^3] \quad \text{for} \quad R < R_0 \equiv R_e{}^{00}$$

$$D(R) = 1 \quad \text{for} \quad R \geq R_0$$

and the constants $A^{\lambda k}$ and $C_8{}^{\lambda k}$ are defined by the values of the depth $\epsilon^{\lambda k}$ and position $R_e{}^{\lambda k}$ of the minimum of $V_{\lambda k}(R)$. The parameters defining the H_2–Ar surface are listed in Table V of ref 6.

For calculations on HD–Ar, the potential surface was transformed to a coordinate system based on the center of mass of HD, which is located $0.1665563536r$ from the bond midpoint. The center of mass transformation introduces Legendre terms of odd order into the potential expansion, so that in the new coordinate sysem the potential is

$$V(R,\xi,\theta) = \sum_{k=0}^{k_{max}} \sum_{\lambda=0}^{\lambda_{max}} \xi^k P_\lambda(\cos \theta) V_{\lambda k}(r)$$

In the present work, the transformation was carried out by using the Gaussian quadrature method of Liu et al,[10] as described by Hutson and Le Roy,[11] with the summations truncated at $\lambda_{max} = k_{max} = 8$.

The diatom matrix elements $\langle v,j|\xi^k|v',j'\rangle$ used to define

(1) See, for example, D. H. Levy, *Adv. Chem. Phys.*, **47**, 323 (1981); T. E. Gough, R. E. Miller, and G. Scoles, *J. Chem. Phys.*, **69**, 1588 (1978); M. P. Casassa, D. S. Bomse, J. L. Beauchamp, and K. C. Janda, *ibid.*, **74**, 5044 (1981).

(2) J. M. Lisy, A. Tramer, M. F. Vernon, and Y. T. Lee, *J. Chem. Phys.*, **75**, 4733 (1981); M. F. Vernon, J. M. Lisy, D. J. Krajnovich, A. Tramer, H. S. Kwok, Y. R. Shen, and Y. T. Lee, *Faraday Discuss. Chem. Soc.*, **73**, 387 (1982).

(3) J. A. Beswick and J. Jortner, *J. Chem. Phys.*, **68**, 2277 (1978); J. A. Beswick and J. Jortner, *Adv. Chem. Phys.*, **47**, 363 (1981); J. A. Beswick and G. Delgado-Barrio, *J. Chem. Phys.*, **73**, 3653 (1980); J. A. Beswick and A. Requena, *ibid.*, **73**, 4347 (1980).

(4) G. E. Ewing, *Chem. Phys.*, **29**, 253 (1978); G. E. Ewing, *J. Chem. Phys.*, **71**, 3143 (1979); G. E. Ewing, *ibid.*, **72**, 2096 (1980); D. A. Morales and G. E. Ewing, *Chem. Phys.*, **53**, 141 (1980).

(5) M. S. Child and C. J. Ashton, *Faraday Discuss. Chem. Soc.*, **62**, 307 (1977); C. J. Ashton, D. Phil. Thesis, Oxford University, 1981.

(6) J. S. Carley, Ph.D. Thesis, University of Waterloo, 1978; R. J. Le Roy and J. S. Carley, *Adv. Chem. Phys.*, **42**, 353 (1980).

(7) A. R. W. McKellar and H. L. Welsh, *J. Chem. Phys.*, **55**, 595 (1971).

(8) I. F. Kidd and G. G. Balint-Kurti, unpublished work.

(9) M. Shapiro, *Isr. J. Chem.*, 11, 691 (1973).

(10) W.-K. Liu, J. E. Grabenstetter, R. J. Le Roy, and F. R. McCourt, *J. Chem. Phys.*, **68**, 5028 (1978).

(11) J. M. Hutson and R. J. Le Roy, *J. Chem. Phys.*, **78**, 4040 (1983). For more details regarding this procedure, see Appendix A of J. M. Hutson and R. J. Le Roy, University of Waterloo Chemical Physics Research Report CP-196.

TABLE I: Level Energies (in cm^{-1}) for H_2, D_2, and HD, Calculated from the Bishop-Shih Potentials for Ground State Molecular Hydrogen

v	j	H_2	D_2	HD
0	0	0.00	0.00	0.00
0	1			89.24
0	2	354.40	179.07	267.10
0	3			532.36
0	4	1168.88	593.74	883.25
0	5			1317.44
0	6	2415.06	1236.57	1832.14
0	7			2424.13
0	8	4052.23	2096.44	3089.84
0	9			3825.39
0	10	6031.35	3159.13	4626.69
1	0	4162.05	2993.96	3632.83
1	1			3718.21
1	2	4498.74	3166.71	3888.37
1	3			4142.14
1	4	5272.33	3566.69	4477.78
1	5			4893.04
1	6	6455.41	4186.67	5385.20
1	7			5951.17
1	8	8008.70	5015.78	6587.45

the potential matrices were generated from exact (numerical) radial wave functions for H_2, D_2, and HD, calculated from smoothed potential curves obtained from the ab initio points of Kołos and Wolniewicz[12] by Bishop and Shih.[13] The diatom vibration–rotation energy levels were also taken from calculations on these potentials, and are listed in Table I.

3. Computational Method

Metastable states were characterized by performing close-coupled scattering calculations for a range of energy values around the energy of the state concerned, and carrying out a simultaneous least-squares fit of resonance parameters to the energy dependence of all the diagonal S-matrix elements.[14] In the close-coupling formulation, a predissociating state appears as a resonant perturbation in the S-matrix eigenphase sum[14,15] $\sigma(E)$, which rises sharply by π across the width of the resonance. Each resonance is characterized by its energy E_m, fwhm width Γ_m, and partial widths Γ_{mi} for each open channel i. The partial widths are related to the total width by

$$\Gamma_m = \sum_i \Gamma_{mi}$$

and the fraction of the predissociation products asymptotically in channel i is given by Γ_{mi}/Γ_m.

The coupled equations were formulated in the space-fixed representation of Arthurs and Dalgarno[16] and solved by using the R-matrix propagator algorithm of Light and Walker.[17] The fundamental constants used here are specified by the single number $\hbar^2/2 = 16.857630$ amu cm^{-1} $Å^2$. The collision reduced masses for H_2–Ar, D_2–Ar, and HD–Ar were taken to be 1.918 865 04, 3.659 342 3, and 2.809 476 2 amu, respectively.

It will be seen below that most of the resonances are extremely narrow ($<<10^{-5}$ cm^{-1}). While this implies that the isolated, narrow resonance approximation is very well satisfied, it also creates severe difficulties in searching for the resonant perturbations in the S matrix. In the present study, this problem was solved by realizing that, on energy scales of say 10^{-5} cm^{-1}, the direct scattering S matrix has an extremely smooth energy dependence. Because of this, it was found possible to detect the "tails" of the resonant Breit–Wigner functions in the S-matrix eigenphase sum[14,15] at up to 10^5 widths away from a resonance. Once such a "tail" has been detected, it is a relatively simple matter to estimate the resonance position and iteratively converge upon it.

TABLE II: Results of Close-Coupling Calculations for $v = 1$, $l = j$, $n = 0$ States of H_2-Ar and D_2-Ar

	H_2-Ar	H_2-Ar	D_2-Ar
$J(p)$	0(+)	1(−)	0(+)
j	0	2	0
E_m/cm^{-1}	4139.076	4478.495	2964.717
$\Gamma_m/10^{-10}$ cm^{-1}	202	983	2.5
$\Gamma_{mj}/10^{-10}$ cm^{-1}			
$j = 0$	2.0		0.07
$j = 2$	18.5	0.66	0.37
$j = 4$	136	17.1	1.25
$j = 6$	45	964	0.85
$j = 8$	<0.01	0.88	0.02

4. Calculations for H_2-Ar and D_2-Ar

The rare gas–molecular hydrogen van der Waals molecules are all weakly anisotropic systems which are well described by space-fixed quantum numbers. The states are characterized by the total angular momentum J, the diatom quantum numbers v and j, the end-over-end angular momentum of the complex l, and the stretching quantum number for the van der Waals bond n. The rigorously conserved quantities are J and the parity label $p = (-)^{j+l+J}$, but the other quantum numbers are also nearly conserved.

For H_2–Ar and D_2–Ar, close-coupling calculations were performed on the lowest state of the complex correlating with vibrationally excited H_2 (D_2). This state has quantum numbers $J(p) = 0(+)$, $v = 1$, $j = 0$, $l = 0$, and $n = 0$. The basis sets used included all diatom rotational levels up to $j = 10$ for $v = 0$ and up to $j = 8$ for $v = 1$. The results are given in the first and third columns of Table II, and are believed to be converged to the precision quoted.

The predissociation width is extremely small for both H_2–Ar and D_2–Ar; the H_2–Ar width corresponds to a lifetime of 0.26 ms, and that for D_2–Ar to a lifetime of 21 ms. Both the smallness of the widths and the relative values for the two systems are consistent with the previous approximate work emphasizing momentum gap effects (see section 1). Surprisingly, however, in both cases the partial widths peak at $j = 4$, with a substantial flux in $j = 6$, despite the absence of terms higher than $P_2(\cos\theta)$ in the potential anisotropy. For this potential, a perturbation theory description of the production of hydrogen in its $v = 0$, $j = 6$ state from a van der Waals complex correlating with H_2 ($v = 1$, $j = 0$) requires at least a third-order treatment. This process would therefore be expected to be strongly disfavored despite the more favorable momentum gap for production of rotationally hot H_2. This point will be discussed in more detail in section 7.

States of H_2–Ar correlating with H_2 in its $v = 1$, $j = 2$ level are energetically capable of predissociating to form H_2 ($v = 1$, $j = 0$), and when allowed this process is very much faster than vibrational predissociation.[18] However,

(12) W. Kołos and L. Wolniewicz, *J. Chem. Phys.*, **41**, 3663 (1964); **43**, 2429 (1965); **49**, 404 (1968); *Chem. Phys. Lett.*, **24**, 457 (1974); *J. Mol. Spectrosc.*, **54**, 303 (1975).

(13) D. M. Bishop and S.-K. Shih, *J. Chem. Phys.*, **64**, 162 (1967).

(14) C. J. Ashton, M. S. Child, and J. M. Hutson, *J. Chem. Phys.*, **78**, 4025 (1983).

(15) A. U. Hazi, *Phys. Rev. A*, **19**, 920 (1979).

(16) A. M. Arthurs and A. Dalgarno, *Proc. R. Soc. London, Ser. A*, **256**, 540 (1960).

(17) J. C. Light and R. B. Walker, *J. Chem. Phys.*, **65**, 4272 (1976); E. B. Stechel, R. B. Walker and J. C. Light, *ibid.*, **69**, 3518 (1978).

(18) R. J. Le Roy, G. C. Corey, and J. M. Hutson, *Faraday Discuss. Chem. Soc.*, **73**, 339 (1982).

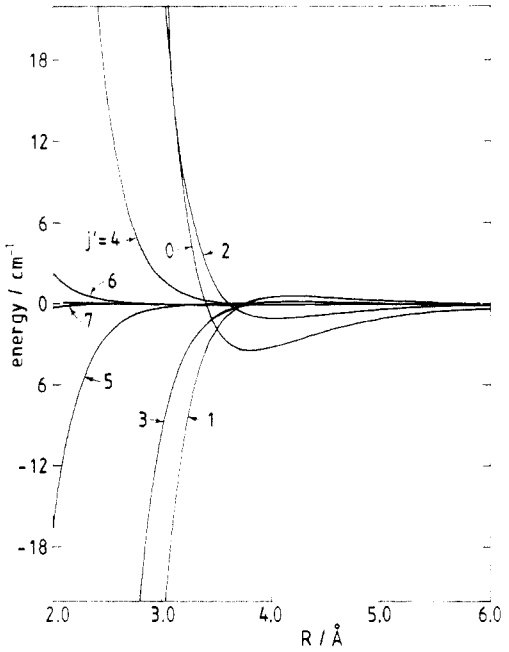

Figure 1. Potential matrix elements between the (v = 1, j = 0) and (v = 0, j') channels for HD–Ar with J = 0. The different coupling functions are labeled with values of j'. Note that the matrix elements include the appropriate Percival–Seaton coefficients, which are responsible for the alternation in sign with j'.

for states with ($j + l + J$) odd there is no j = 0 channel, so that v = 1, j = 2 states with p odd must again predissociate vibrationally. Since the H_2 molecule in the van der Waals complex is already in a j = 2 state, processes yielding H_2 in high j levels would be expected to be more favorable here than would be the case for complexes formed from H_2 (j = 0), because of the more direct potential coupling. We have therefore performed calculations on the $J(p)$ = 1(−) state of H_2–Ar correlating with (v = 1, j = 2), and the results obtained are shown in Table II. The j = 6 predissociation channel is now even more important than before, and the total level width is an order of magnitude larger than for the J = 0, j = 0 state discussed above.

The most striking feature of all the results presented above is that the fragments are produced mainly in highly excited rotational states which are not directly coupled to the predominant component of the bound state by the intermolecular potential used here. The *real* intermolecular potential, however, will contain anisotropic terms of higher order than $P_2(\cos\theta)$, which can couple the high j open channels directly to the low j closed channels. These terms may significantly enhance both the total predissociation rates and the proportion of the fragments in highly excited rotational states.

5. Calculations for HD-Ar

The center of mass transformation for HD–Ar not only introduces a $P_1(\cos\theta)$ anisotropy into the intermolecular potential, but also yields nonzero high-order Legendre terms. The near-resonant v = 0 channels (i.e., those of high j) are now directly coupled to the zeroth order v = 1 channels, albeit weakly, so that the probability of predissociation to these channels is much greater than for H_2–Ar or D_2–Ar. The direct matrix elements of the intermolecular potential coupling the v = 1, j = 0 and v' = 0, j' channels for J = 0 are shown in Figure 1. The matrix elements decrease rapidly in magnitude as the open channel j' value increases, but even for high j' the coupling terms are significant at short distances. The present HD–Ar model system should thus be more realistic in its VP behavior than either the H_2–Ar or D_2–Ar models, since the potential anisotropy is not artificially restricted to low-order Legendre terms.

TABLE III: Results of Close-Coupling Calculations for HD–Ar[a]

j	0	2
E_m/cm^{-1}	3606.322	3863.786
Γ_m/cm^{-1}	15.6×10^{-9}	39.6×10^{-8}
Γ_{mvj}/cm^{-1}		
(v,j) = (0,0)	0.4×10^{-9}	1.2×10^{-8}
(v,j) = (0,1)	1.0×10^{-9}	3.3×10^{-8}
(v,j) = (0,2)	1.2×10^{-9}	4.7×10^{-8}
(v,j) = (0,3)	1.2×10^{-9}	4.8×10^{-8}
(v,j) = (0,4)	1.8×10^{-9}	3.3×10^{-8}
(v,j) = (0,5)	2.0×10^{-9}	1.0×10^{-8}
(v,j) = (0,6)	0.3×10^{-9}	0.3×10^{-8}
(v,j) = (0,7)	3.7×10^{-9}	4.9×10^{-8}
(v,j) = (0,8)	4.0×10^{-9}	14.7×10^{-8}
(v,j) = (0,9)		1.2×10^{-8}

[a] Both resonances are v = 1, J = 0, n = 0.

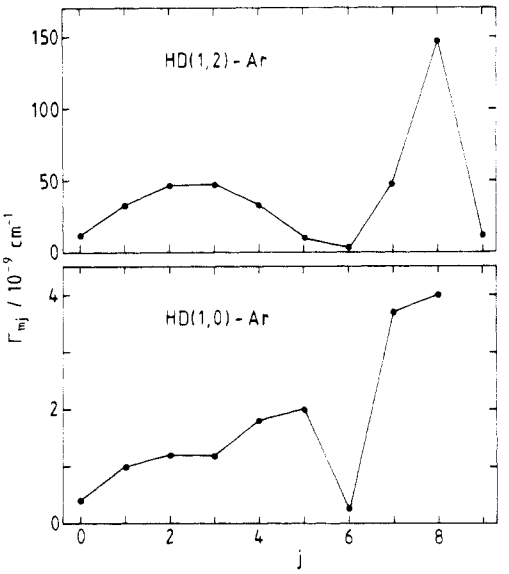

Figure 2. Partial widths for vibrational predissociation of HD(v,j)–Ar. The results for HD(1,2)–Ar were obtained by using a basis set excluding the (v = 1, j = 0) and (v = 1, j = 1) channels.

Close-coupling calculations for the lowest state of HD–Ar correlating with HD (v = 1, j = 0) yielded the results given in the first column of Table III and the lower part of Figure 2. The basis set used included all HD v = 0 states up to j = 10, and all v = 1 states up to j = 8. It may be seen that the partial widths peak at j = 5, drop to a much smaller value for j = 6, and then increase again for the j = 7 and j = 8 channels. Thus there is a clear near-resonant contribution to the vibrational predissociation of HD–Ar, with about half the products appearing in the highest two channels.

For near-resonant dominated VP, one expects that both the product diatom rotational state distribution and the total VP width will be very sensitive to the difference between the metastable level energy and the open channel threshold of highest energy. The (v = 0, j = 8) channel for predissociation of HD(1,0)–Ar is not very strongly near-resonant, since its threshold lies more than 500 cm^{-1} below the resonance energy. It is thus interesting to seek a case where there is a closer near-resonance. This occurs for states of HD–Ar correlating with HD (v = 1, j = 2), where the $J(p)$ = 0(+) state lies only 38.8 cm^{-1} above the v = 0, j = 9 threshold. The full treatment of this state is complicated by the presence of the (v = 1, j = 0) and (v

TABLE IV: Dependence of Partial Widths on the Closed Basis Set[a]

j_{max} ($v = 1$)	0	2	4	6	8
$\Gamma_m/10^{-10}$ cm^{-1}	518	1391	252	202	202
$\Gamma_{mj}/10^{-10}$ cm^{-1}					
$j = 0$	12.0	2.8	2.0	2.0	2.0
$j = 2$	96	39.3	18.7	18.5	18.5
$j = 4$	343	630	137	136	137
$j = 6$	67	718	94	45	45
$j = 8$	<0.01	<0.01	0.07	<0.01	<0.01

[a] Calculations are for the $v = 1, j = 0, n = 0$ $J(p) = 0(+)$ state of H_2-Ar, using an open channel basis set with j_{max} ($v = 0$) = 8.

TABLE V: Dependence of Partial Widths on the Open Channel Basis Set[a]

j_{max} ($v = 0$)	0	2	4	6	8	10
$\Gamma_m/10^{-10}$ cm^{-1}	0.4	9.7	162	204	202	202
$\Gamma_{mj}/10^{-10}$ cm^{-1}						
$j = 0$	0.4	1.2	1.9	2.0	2.0	2.0
$j = 2$		8.5	17.0	18.4	18.5	18.5
$j = 4$			143	137	137	136
$j = 6$				46	45	45
$j = 8$					<0.01	<0.01

[a] Calculations are for the $v = 1, j = 0, n = 0, J(p) = 0(+)$ state of H_2-Ar, using a closed channel basis set with j_{max} ($v = 1$) = 8.

= 1, j = 1) open channels, which allow fast rotational predissociation of HD(1,2)–Ar in addition to the much slower vibrational predissociation.[11] The partial widths for these two channels are 0.33 and 1.07 cm^{-1}, respectively, and the necessity of fitting the nonresonant part of the S matrix over such a large energy range makes it very difficult to characterize the small partial widths for the vibrationally inelastic channels.

In order to investigate the effect of a very close near-resonance on VP, we have performed calculations for HD(1,2)–Ar excluding the ($v = 1, j = 0$) and ($v = 1, j = 1$) channels, but otherwise using the same basis set as for HD(1,0)–Ar. The results are shown in column 2 of Table III and in the upper part of Figure 2. Once again, the partial widths show a bimodal dependence on j, with a minimum at $j = 6$. It is striking that the minimum appears at the same j value here as for HD(1,0)–Ar, although the total width is a factor of 20 larger than in that case.

There are two possible explanations of the bimodal distribution. The first is that there are two different predissociation mechanisms responsible for the two peaks. The peak at low j probably results from high-order processes involving multiple couplings through low-order Legendre polynomials. This mechanism may be viewed as involving initial predissociation to low j open channels (mainly $j = 0$, 1, and 2), followed by further energy redistribution caused by couplings among the open channels. High-order effects are certainly responsible for the $j = 4$ and $j = 6$ products in the H_2–Ar and D_2–Ar systems, where only a $P_2(\cos\theta)$ anisotropy is present. The peak at high j would then result from direct coupling between the closed channels and the open channels concerned, involving high-order Legendre terms in the anisotropy. For the potential surfaces used here, this mechanism can occur only for HD–Ar, and the strength of the peak at high j may be expected to depend sensitively on the high-order terms in the potential.

An alternative explanation of the bimodal distribution is that it results from a rotational rainbow effect. This possibility will be discussed in section 9.

6. Basis Set Dependence

It was found that the calculated predissociation widths were very sensitive to the basis sets used, and convergence with respect to basis set size was much slower than anticipated. A systematic study of the dependence of the parameters of the H_2–Ar $J = 0$ resonance on both closed and open channel basis sets was therefore undertaken; the results are summarized in Tables IV and V.

Table IV shows the widths and partial widths obtained with different *closed* channel basis sets, using a converged open channel basis set with j_{max} ($v = 0$) = 8. It may be seen that the widths fluctuate wildly for small closed channel basis sets, becoming stable only at j_{max} ($v = 1$) = 6; for example, introducing the $j = 4$ closed channel decreases the total width by a factor of 5, even though $j = 4$ is not directly coupled to the zeroth-order bound-state channel ($j = 0$). This does not augur well for the utility of perturbation theory, since it indicates that a very accurate representation of the closed channel wave function will be required before any perturbative scheme can be expected to give accurate results.

A further unexpected feature is the dependence of the high j partial widths on the closed channel basis set. The fluxes into the $j = 6$ and 8 open channels reach a maximum for j_{max} ($v = 1$) = 2 and 4, respectively, and then decline again as more closed channels are added. This is surprising, since the partial widths for the high j open channels would be expected to be dominated by contributions from closed channels with similar j values. Similar behavior was observed for D_2–Ar and HD–Ar.

The convergence with respect to the *open* channel basis set, shown in Table V, is also somewhat surprising. The introduction of additional open channels of low j does not simply add a new independent predissociation mechanism, but also violently perturbs the partial widths for energetically nearby channels that are already open. This indicates that coupling between the different low j open channels is important, and any successful perturbation scheme must take account of this. On the other hand, Table V shows that introducing extra open channels of high j has relatively little effect. This presumably reflects weaker open-open channel coupling because of the large energy spacing of the channel asymptotes at high j.

Although the physical reason for these strange convergence effects in such a weakly coupled system is not clear, the most plausible explanation lies in the oscillatory cancellation effects mentioned in section 1. In a diabatic representation of the scattering problem, each partial width may be written as the square of a matrix element of the intermolecular potential between a multichannel bound state wave function and the continuum wave function for the channel concerned.[19] If such a matrix element has extensive oscillatory cancellation along the intermolecular distance coordinate, its overall value can be expected to be very sensitive to small changes in the shape and composition of the wave functions. Thus, changes in basis set which alter the wave functions only slightly could have a greatly exaggerated effect on the VP widths and partial widths.

The oscillatory cancellation occurring in VP is illustrated in Figure 3 for the predissociation of $H_2(1,0)$–Ar to form $H_2(0,0)$. The top section of the figure shows the effective potential for the $v = 1, j = 0$ channel, and the zeroth order $n = 0$ bound state wave function supported by this potential. The central section of the figure shows the effective potential for the $v = 0, j = 0$ open channel, and the

(19) U. Fano, *Phys. Rev.*, **124**, 1866 (1961).

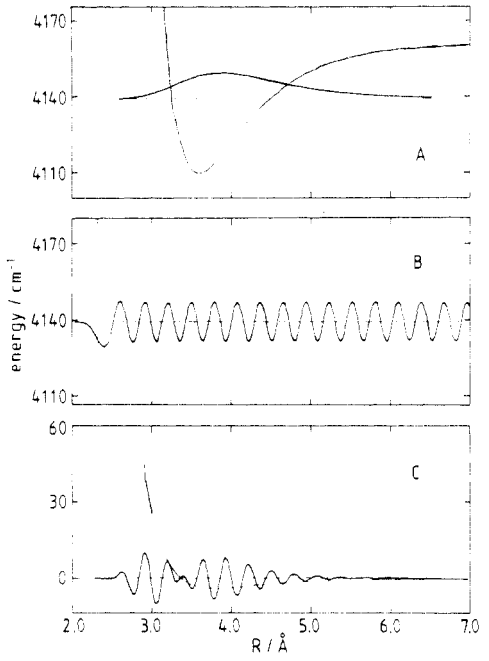

Figure 3. Effective potential curve and wave function for the closed channel (section A) and open channel (section B), and the off-diagonal coupling function and golden rule matrix element (section C) for predissociation of $J = 0$ $H_2(1,0)$–Ar to yield H_2 ($v = 0$, $j = 0$).

continuum wave function at the energy of the bound state. Finally, the lowest section shows the off-diagonal potential matrix element coupling the two channels and the integrand of the golden rule width expression. It may be seen that the integrand is highly oscillatory, and the value of the full integral is only about 10^{-4} of the area of a single loop in the integrand.

7. Perturbation Theory Calculations

The results of section 6 make it clear that no simple perturbative scheme can be expected to give quantitatively accurate vibrational predissociation widths for the rare gas–molecular hydrogen van der Waals complexes. However, we have previously found[14] that comparison of perturbative and close-coupling results provides important insights into the physics of predissociation in van der Waals complexes. It is therefore desirable to investigate whether perturbation theory can give qualitatively useful information on the relative predissociation widths for different quantum states and isotopic species in the present case.

The simplest possible perturbative scheme is the space-fixed distortion (SFD) method, which gives good results for states of H_2–Ar predissociating by internal rotation.[18] In this method, the bound-state part of the wave function is represented as

$$\psi^{\mathrm{SFD}}_{vjlJ}(\mathbf{R},\mathbf{r}) = r^{-1}R^{-1}\phi_{vj}(r)\Phi^{J}_{jl}(\hat{R},\hat{r})\ \chi^{\mathrm{SFD}}_{vjl}(J|R)$$

where $\phi_{vj}(r)$ is the stretching wave function of the diatom, $\Phi^{J}_{jl}(\hat{R},\hat{r})$ is the space-fixed angular function for the (j,l)th channel, and $\chi^{\mathrm{SFD}}_{vjl}(J|R)$ is the solution of the one-dimensional Schrödinger equation

$$\left[-\frac{\hbar^2}{2\mu}\frac{\mathrm{d}^2}{\mathrm{d}R^2} + U^{vjvj}_{ll}(J|R) - E^{\mathrm{SFD}}_{vjlJ}\right]\chi^{\mathrm{SFD}}_{vjl}(J|R) = 0$$

The width of the predissociating level in this formulation is given by the golden rule expression

$$\Gamma_m = \sum_i \Gamma_{mi} = \sum_{v''j''\eta''} \left| \int \chi^{(0)}_{v''j''\eta''}(J|R)\ U^{v''j''v''j}_{l''l}(J|R)\chi^{\mathrm{SFD}}_{vjl}(J|R)\ \mathrm{d}R\right|^2$$

where the summation runs over all open channels, $\chi^{(0)}_{v''j''\eta''}(J|R)$ is the regular single-channel continuum wave function associated with open channel (v'',j'',l''), and $U^{v''j''v''j}_{l''l}(J|R)$ is the matrix element of the interaction potential coupling open channel (v'',j'',l'') to closed channel (v,j,l).

The level energies and widths obtained by using the SFD approximation are shown in the upper part of Table VI.

TABLE VI: Results of Perturbative Calculations for Vibrational Predissociation[a]

	H_2–Ar	H_2–Ar	D_2–Ar	HD–Ar
	Space-Fixed Distortion Results			
(j,l,J)	(0,0,0)	(2,2,1)	(0,0,0)	(0,0,0)
E_m/cm^{-1}	4139.107	4478.500	2964.755	3606.750
$\Gamma_m/10^{-10}$ cm^{-1}	30.1	26.9	0.86	8.4
$\Gamma_{mj}/10^{-10}$ cm^{-1}				
$j = 0$	0.6		0.06	0.04
$j = 1$				2.4
$j = 2$	29.5	0.07	0.80	3.7
$j = 3$				1.5
$j = 4$		26.8		0.51
$j = 5$				0.13
$j = 6$				0.04
$j = 7$				0.02
$j = 8$				0.02
	Second-Order Perturbation Theory Results			
(j,l,J)	(0,0,0)	(2,2,1)	(0,0,0)	(0,0,0)
E_m/cm^{-1}	4139.075	4478.494	2964.716	3606.317
$\Gamma_m/10^{-10}$ cm^{-1}	649	3536	10.9	2536
$\Gamma_{mj}/10^{-10}$ cm^{-1}				
$j = 0$	0.6		0.00	0.3
$j = 1$				107
$j = 2$	74	0.3	2.1	85
$j = 3$				203
$j = 4$	575	75	8.8	397
$j = 5$				542
$j = 6$		3461		548
$j = 7$				440
$j = 8$				214

[a] All resonances are for $v = 1$, $n = 0$ states.

The total widths are grossly too small, and the degree of rotational excitation of the diatom products is greatly underestimated. This clearly confirms that the mechanism of VP in these systems is dominated by high-order potential couplings rather than by the direct zeroth-order bound–continuum couplings considered in the SFD approximation. Note that the level energies obtained from the SFD approximation are also somewhat in error, since all level shifts due to off-diagonal couplings are neglected.

The results of section 6 suggest that the most serious failing of the SFD approximation lies in its inadequate representation of the bound state part of the wave function. The contributions of higher j ($v = 1$) closed channels to this function clearly play a major role in determining the partial widths to the important high j open channels. Thus the next level of sophistication is to use the SFD wave function as a zeroth-order approximation, and to introduce the other closed channels by perturbation theory. The bound-state part of the wave function is then represented

$$\psi_{vjlJ} = \psi^{\mathrm{SFD}}_{vjlJ} + \sum_{v'l'j'} r^{-1}R^{-1}\phi_{v'j'}(r)\Phi^{J}_{j'l'}(\hat{R},\hat{r})\ \chi^{(1)}_{v'j'l'}(J|R)$$

where the summation runs over all *closed* channels. The first-order correction functions $\chi^{(1)}_{v'j'l'}(J|R)$ are obtained as solutions of the uncoupled inhomogeneous differential equations[20]

$$\left[-\frac{\hbar^2}{2\mu}\frac{\mathrm{d}^2}{\mathrm{d}R^2} + U^{v'j'v'j'}_{l'l'}(J|R) - E^{\mathrm{SFD}}_{vjlJ}\right]\chi^{(1)}_{v'j'l'}(J|R) = -U^{v'j'vj}_{l'l}(J|R)\chi^{\mathrm{SFD}}_{vjl}(J|R)$$

and thus include all contributions from both bound and continuum levels of the perturbing channels. The second-order energy shifts due to the other closed channels are given by

$$E^{(2)}_{vjl} = \sum_{v'j'l'}\int \chi^{\mathrm{SFD}}_{vjl}(J|R)\ U^{vjv'j'}_{ll'}(J|R)\chi^{(1)}_{v'j'l'}(J|R)\ \mathrm{d}R$$

and the widths and shifts due to the open channels may be calculated by using the Green's function method described in section 5 of ref 14.

The level energies, widths, and partial widths obtained from this second scheme are given in the lower part of Table VI. For H_2–Ar and D_2–Ar, the total widths given by this approximation are larger than the true widths by a factor of 3 to 4, but the dominant predissociation channel is correctly predicted in each case, as are the isotope effects. The method fails to give any transitions with $\Delta j > 4$ because the bound-state wave function contains no contributions from $|j' - j| > 2$; however, the failure is not as serious as for the SFD approximation. For HD–Ar, the total and partial widths are too large by a factor of around 15, and the perturbation theory approach incorrectly predicts a peak in the partial widths at $j = 6$. This failure is probably still due to an inadequate representation of the bound-state wave function, but it is surprising that the error is so large.

It is clear that the results obtained from perturbation theory are very sensitive to the quality of the bound-state wave function used, and it has already been remarked in section 6 that continuum–continuum coupling must play a significant role. It is likely that the perturbation theory results could be improved by using a more sophisticated closed channel representation, but the very strong basis set dependence of the widths and partial widths discussed in section 6 underlines the limited accuracy achievable with perturbation theory for these systems.

(20) J. M. Hutson and B. J. Howard, *Mol. Phys.*, 41, 1113 (1980).

TABLE VII: Results of Close-Coupling Calculations for the $v = 1, j = 0, n = 0, J(p) = 1(+)$ State of H_2–Ar

E_m/cm^{-1}	4140.191
$\Gamma_m/10^{-10}\ \mathrm{cm}^{-1}$	244
$\Gamma_{mj}/10^{-10}\ \mathrm{cm}^{-1}$	
$j = 0$	1.9
$j = 2$	18.2
$j = 4$	133
$j = 6$	91
$j = 8$	0.07

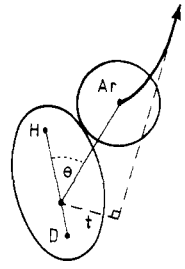

Figure 4. The classical picture of predissociation. The heavy arrow represents a curved classical trajectory, and t is the length of the effective moment arm.

8. Comparison with Photodissociation Calculations

In order to make comparisons with the photodissociation calculations of Kidd and Balint-Kurti,[8] we have performed calculations for the lowest vibrationally predissociating $J(p) = 1(+)$ state of H_2–Ar; the results obtained are shown in Table VII. This calculation used a basis set of H_2 rotational levels with $j_{max} = 8$ for $v = 0$ and $j_{max} = 4$ for $v = 1$, which is the same size as that used in ref 8; for the $J(p) = 0(+)$ state this basis set gives a width which is about 20% too large, mainly because it overestimates the partial widths to the $j = 6$ and 8 channels. The total and partial widths for the $J(p) = 1(+)$ state are about 3% lower than those obtained for the 0(+) state with the same basis set, probably because of centrifugal effects.

Within the isolated narrow resonance approximation, the level width obtained by fitting the S-matrix eigenphase sum to the Breit–Wigner formula should be the same as that obtained by fitting calculated photodissociation cross sections to a Lorentzian (or Fano–Beutler[19]) line shape.[5] This is indeed found: our width of $2.44 \times 10^{-8}\ \mathrm{cm}^{-1}$ compares well with Kidd and Balint-Kurti's value of $2.45 \times 10^{-8}\ \mathrm{cm}^{-1}$, and our partial widths also agree well with their partial cross sections. This confirms that the level widths and product state populations obtained from scattering calculations of the type used here are the same as those measured in a spectroscopic experiment.

9. Classical Mechanics and Rotational Rainbows

Up to this point the predissociation results have been discussed entirely in terms of quantum mechanics. However, certain features of the rotational distributions suggest classical explanations. Consider a van der Waals molecule commencing vibrational predissociation from an initial configuration on the repulsive wall of the potential surface. The vibrational energy of the diatom must be converted into rotational and translational energy of the fragments, conserving energy and angular momentum. The fragments are initially at rest with respect to one another, and are driven apart by the intermolecular potential as shown in Figure 4; note in particular that, because of the potential

anisotropy, the acceleration is not necessarily along the line of centers, but may be considered to originate at a point displaced from the diatom center of mass by a moment arm of length t. If the final relative momentum in the outgoing channel is k, where

$$k^2 = \frac{2\mu}{\hbar^2}(E - E_j)$$

then by conservation of angular momentum the change in the rotational quantum number of the diatomic fragment is

$$\Delta j = kt$$

Conversely, we may estimate the moment arm length t_j required to produce fragments in rotational state j

$$t_j = \Delta j\left(\frac{\hbar^2}{2\mu(E - E_j)}\right)^{1/2}$$

If the time required for the fragments to separate is short compared to the period of rotation of the diatomic molecule, the predissociation effectively occurs at a fixed value of the orientation angle θ. The length of the moment arm t is a function of θ: it is zero for $\theta = 0$ and π, and for homonuclear diatomics for $\theta = \pi/2$ also. Between these angles, $t(\theta)$ passes through a maximum, so that a range of angles around θ_{max} cause nearly the same degree of rotational excitation. This gives rise to a singularity in the classical rotational distribution at the associated value of Δj, and an oscillatory "rainbow" structure in the quantal distribution. Rotational rainbows have been the subject of much theoretical work in the context of rotationally inelastic scattering.[21]

It is tempting to suggest that the bimodal rotational distribution observed for VP in HD–Ar (Figure 2) is a rotational rainbow phenomenon. If this is the case, the rainbow angular momentum transfer corresponds to $\Delta j \approx 8$, giving $t_{max} \approx 1$ Å; this value is too large for HD–Ar in a hard wall model, since the HD bond length is itself only 0.78 Å. However, the anisotropy of the attractive part of the potential could give rise to additional angular momentum transfer, so that a rotational rainbow remains a possible source of the oscillatory structure in Figure 2. Even if the oscillatory structure observed here is not a rainbow phenomenon, there can be little doubt that rotational rainbows will cause oscillatory rotational distributions for predissociation of van der Waals molecules with larger reduced masses or smaller monomer rotational constants.

10. Conclusion

Using the most realistic potential surface available, we have performed close-coupling calculations of level energies and widths for vibrationally predissociating states of the H_2–Ar, D_2–Ar, and HD–Ar van der Waals complexes. These are exact results for the present model problem. Our results agree well with photodissociation calculations currently being performed by other workers. The calculated level widths are small, and it would not be possible to measure them (or the corresponding lifetimes) with current experimental capabilities.

By investigating the convergence of the close-coupling calculations and by comparison with perturbative results, we have shown that the predissociation mechanism is dominated by high-order potential couplings, so that perturbation theory cannot successfully reproduce the exact results. This is a remarkable finding because the H_2–Ar systems are conventionally considered to be weakly coupled. We suggest the general explanation that this effect is due to oscillatory cancellation in integrals over the intermolecular distance coordinate.

The major influence of the high-order couplings is that predissociation predominantly produces rotationally hot H_2, D_2, or HD. Because such transitions have a smaller momentum gap than for production of rotationally cold diatoms, this effect greatly increases the VP widths. Perturbation calculations considering only direct potential couplings were shown to predict predominant production of rotationally cold diatoms and to give total widths drastically below the true values. The near-resonant effect was found to be greatest for HD–Ar, because of the extra angular terms introduced into the intermolecular potential by the diatom center of mass shift.

These results have important implications for the study of VP in other systems. Following the discussion in section 1, one would expect that a near-resonant vibration-to-rotation energy transfer effect in VP would be favored by large rotational constants of the monomer fragments and by a strongly anisotropic intermolecular potential. Since we have found a strong effect even in the weakly anisotropic H_2–Ar systems, it seems probable that near-resonant effects will dominate the VP of more strongly coupled complexes such as HCl–Ar, HF–Ar, or $(HF)_2$. This conclusion disagrees markedly with earlier predictions of near-resonant effects,[5] which neglected high-order potential couplings. It now seems quite possible that the near-resonant width enhancement will be sufficiently great that the VP widths for such systems will be experimentally measurable. This suggestion has recently received confirmation from experimental work on the infrared spectroscopy[22] and photodissociation dynamics[2] of $(HF)_2$; the infrared spectra show line widths up to 10^{-2} cm^{-1} attributed to vibrational predissociation, while in the photofragmentation experiments it appears that HF fragments appear with very low translational energy and hence high rotational excitation.

Acknowledgment. The authors are grateful to Mr. I. F. Kidd and Dr. G. G. Balint-Kurti for supplying details of their photodissociation calculations on H_2–Ar in advance of publication, and to Dr. H. R. Mayne for comments on the manuscript.

Registry No. Ar, 7440-37-1; H_2, 1333-74-0; D_2, 7782-39-0; HD, 13983-20-5.

(21) W. Schepper, U. Ross, and D. Beck, *Z. Phys. A*, **290**, 131 (1979); R. Schinke and P. McGuire, *J. Chem. Phys.*, **71**, 4201 (1979); R. Schinke, W. Müller, and W. Meyer, *ibid.*, **76**, 895 (1982).

(22) A. S. Pine and W. J. Lafferty, *J. Chem. Phys.*, **78**, 2154 (1983).